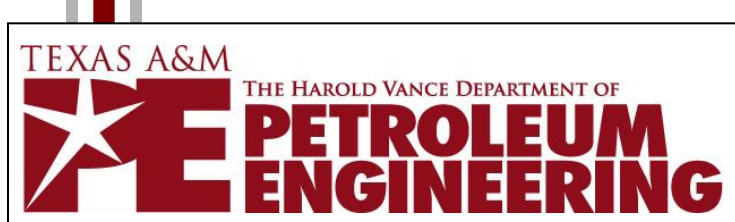


Prediction of fracture initiation pressure and fracture geometries in elastic isotropic and anisotropic formations

Presenter: Han Li

Advisor: Dr. Christine Ehlig-Economides

2/27/2015



Outline

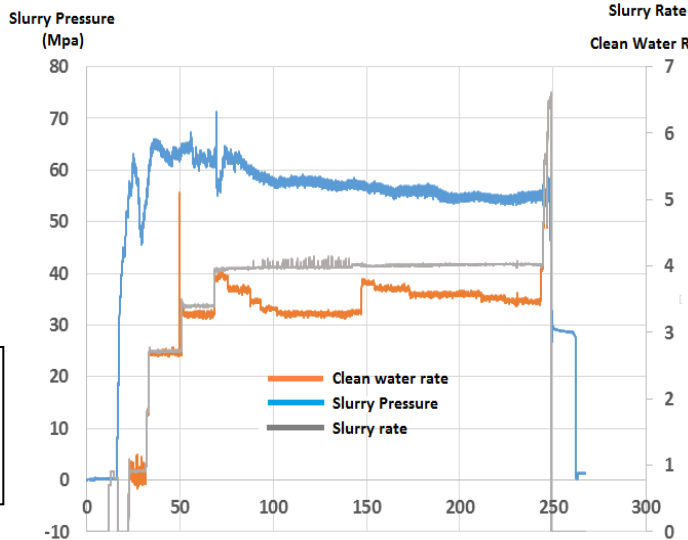
- Introduction
- Simulation Methods
- Results and Discussions
- Conclusions



Introduction

Field data observation:

- (1). The large pressure fluctuations for both downhole pressure and surface pressure before proppant reach the port.
- (2). Large variations in fracturing pressures for different stages.
- (3). The blockage of proppant transport as evidenced by the increase in pressure when proppant enter the fracture.



Pumping rate and pressure plot for stage 17 of a well in Horn River field data

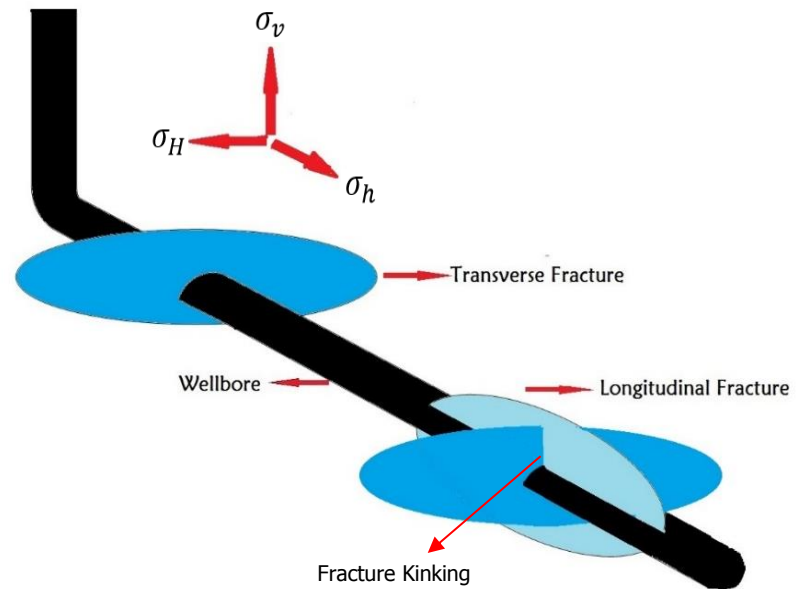
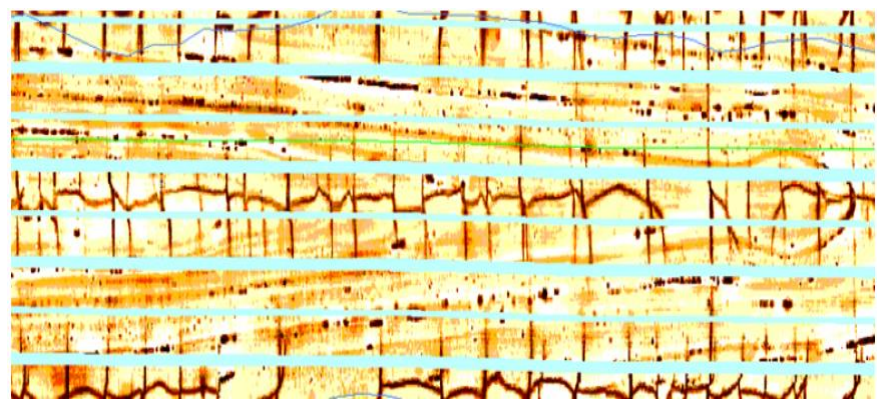


Diagram of near-wellbore fracture complexity and reorientation from longitudinal fractures to transverse fractures



Waters et al (2006). Image log of a Barnett horizontal well drilled in the direction of the minimum horizontal stress showing fractures in both longitudinal and transverse directions (dark colors)

Introduction

- Elastic anisotropic properties of shale formation

Transverse isotropy: **E_v, E_h, V_v, V_h, G**

Affects four key geomechanical steps:

1. The in-situ stress field
2. The stress concentration around the borehole
3. Failure properties both in tension and compression
4. Fracture geometries

- Well deviation

Near wellbore stresses is calculated by:

P_b , θ_{inc} , θ_{az} , σ_h , σ_H and σ_v .

Results: σ_{xx} , σ_{yy} , σ_{zz} and σ_{xy}

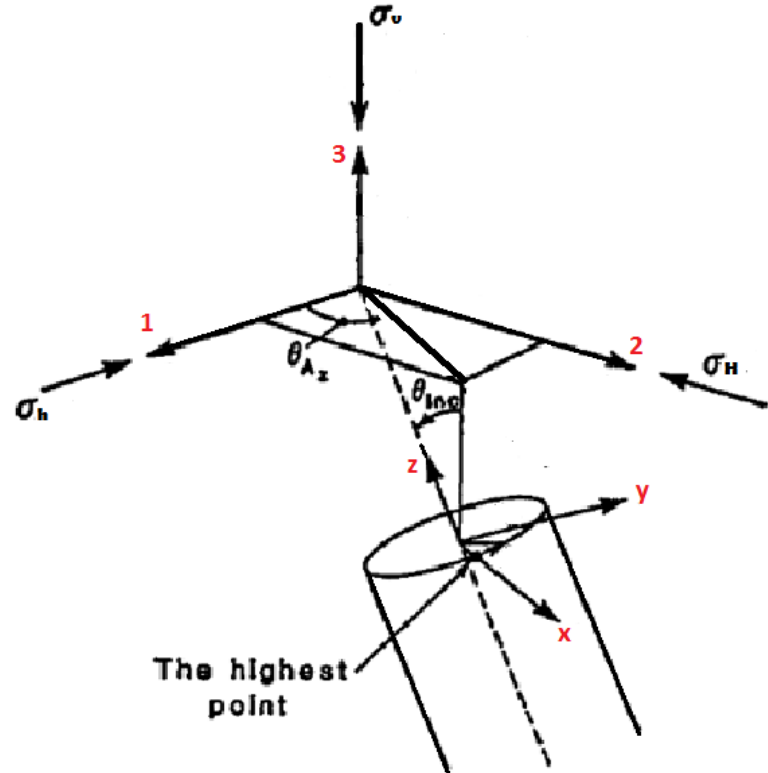
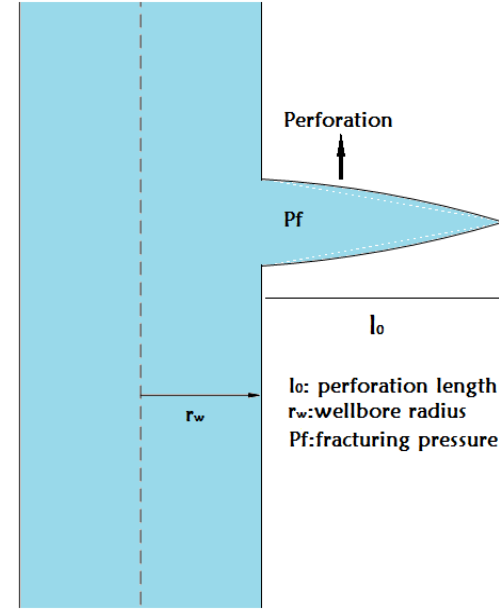


Diagram of deviated well in global coordinate (1, 2, 3) and local coordinate (x, y, z)

Simulation Methods

Based on **linear fracture mechanics theory** to study the effect of perforation geometry on initiation fracture patterns:



$$\frac{K_I}{\sqrt{\pi l}} = \frac{2}{\pi} \int_0^{l_0} p(x + r_w) f\left(\frac{x}{l_0}, \frac{l_0}{r_w}\right) \frac{dx}{l_0 \sqrt{1 - (\frac{x}{l_0})^2}} \quad (1)$$

$$f(x/l_0, l_0/r_w) = \left(\frac{x/l_0 + r_w/l_0}{1 + r_w/l_0} \right)^{d-1} [1 + 0.3(1 - \frac{x}{l_0})(\frac{1}{1 + l_0/r_w})^4] \quad (2)$$

$$d = \begin{cases} 1 & \text{for longitudinal fracture} \\ 2 & \text{for transverse fracture} \end{cases} \quad (3)$$

For net pressure $p(x+a)$:

$$P(x + r_w) = P_f - \sigma_c(x + r_w) \quad (4)$$

Calculation of clamping stress $\sigma_c(x + a)$:

$$\sigma_c(x + r_w) = \begin{cases} \sigma_{zz}^\infty - \nu * [(\sigma_{xx} - \sigma_{yy}) * \cos(2\theta) + 4 * \sigma_{xy} * \sin(2\theta)] \\ \frac{r_w^2}{r^2} * P_b + \frac{\sigma_{xx} + \sigma_{yy}}{2} * \left(1 + \frac{r_w^2}{r^2}\right) - \frac{\sigma_{xx} - \sigma_{yy}}{2} * \left(1 + 3 * \frac{r_w^4}{r^4}\right) * \cos(2\theta) - \sigma_{xy} * (1 + 3 * \frac{r_w^4}{r^4}) * \sin(2\theta) \end{cases} \quad (5)$$

$$5(6)$$

Simulation Methods

Equations for elastic isotropic and anisotropic formations

- Overburden stress:

$$\sigma_v = g * \int_0^z \rho(z) dz \quad (7)$$

- For elastic isotropic formations:

$$\sigma_H = K_{iso} * (\sigma_v - \alpha P_p) + \alpha P_p + \sigma_{H,Tectonic} \quad (8)$$

$$\sigma_h = K_{iso} * (\sigma_v - \alpha P_p) + \alpha P_p + \sigma_{h,Tectonic} \quad (9)$$

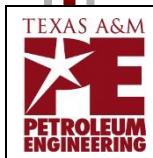
$$K_{iso} = \frac{v}{1-v} \quad (10)$$

- For elastic anisotropic formations:

$$\sigma_H = K_{aniso} * (\sigma_v - \alpha P_p) + \alpha P_p + \sigma_{H,Tectonic} \quad (11)$$

$$\sigma_h = K_{aniso} * (\sigma_v - \alpha P_p) + \alpha P_p + \sigma_{h,Tectonic} \quad (12)$$

$$K_{aniso} = \frac{E_h}{E_v} * \frac{v_v}{1-v_h} \quad (13)$$



Simulation Methods

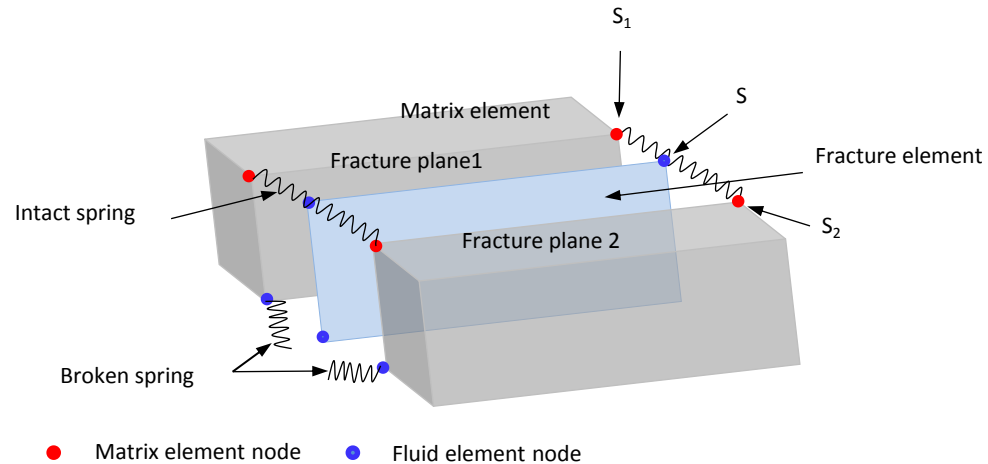
Developed 2D Finite element-Discrete element method (FEDEM) code

Spring: stress and strain delivery

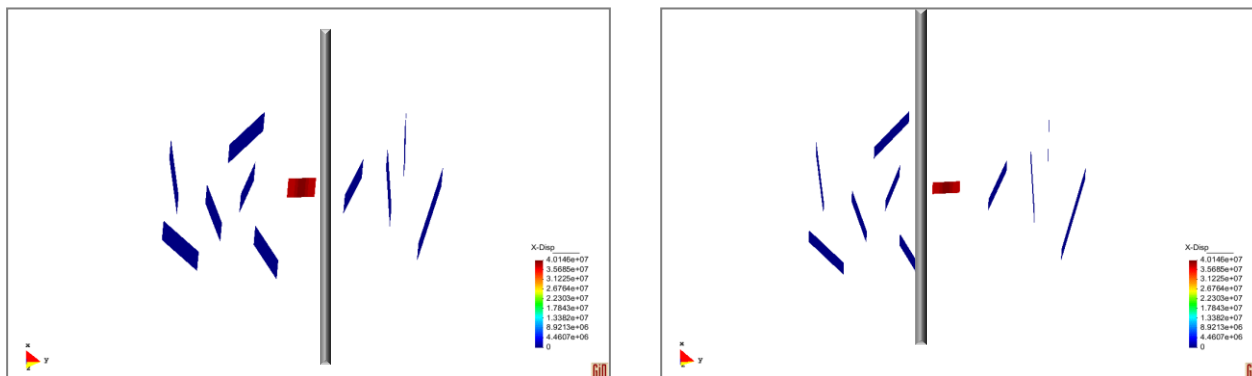
Failure of spring: creation of a fracture element between matrix elements

Model functionality:

1. Interaction between hydraulic fractures and natural fractures.
2. Simulating multi-fractures propagation in multi-well scheme.
3. Consider formation plastic properties



Schematic of combined model of Finite Element Method and Discrete Element Method



Results and Discussions

- Field data:

	σ_v (psi)	σ_H (psi)	σ_h (psi)	P _p (psi)	r_w (ft)	Biot's coefficient	K _{IC} (psi*inch ^{0.5})	V _h	V _v
Marcellus	6780	5932.5	5085	4068	0.35	0.7	1200	0.17	0.26
Fayetteville	5650	5085	4520	2542.5	0.35	0.7	1200	0.2	0.24

- Eight simulation cases:

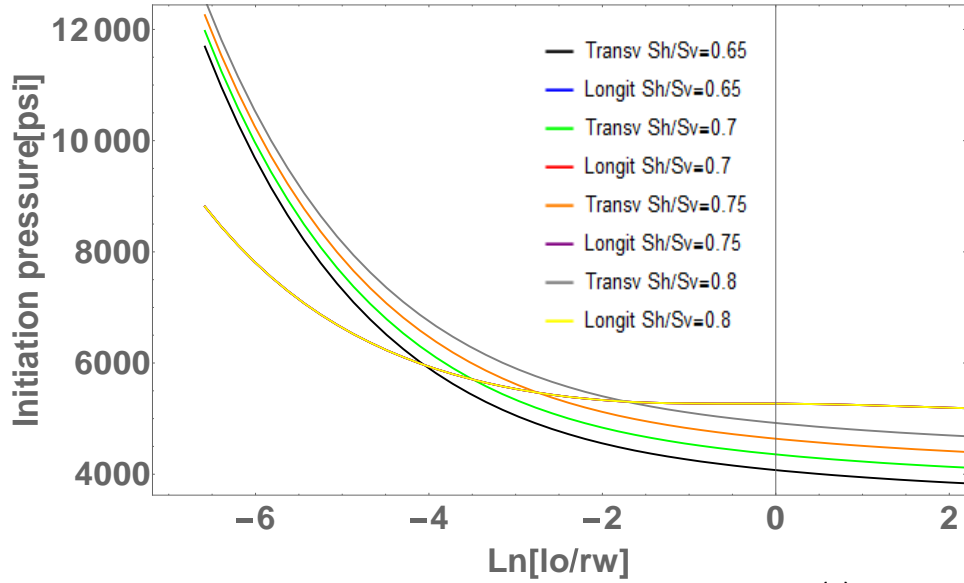
Case number	Object	Formation type	Range	Regimes
1	σ_h	Isotropic	$\sigma_h/\sigma_v: 0.8-0.75-0.7-0.65$	Normal fault
2	σ_H	Isotropic	$\sigma_H/\sigma_v: 0.95-0.9-0.85-0.8$	Normal fault
3	σ_v	Isotropic	$\sigma_v/\sigma_H: 1.1-1.05-1.0-0.95-0.9$	Strike-Slip & Normal fault
4	Eh/Ev	Anisotropic	Eh/Ev: 1-1.2-1.4-1.6	Normal fault
5	Kaniso/Kiso	Anisotropic	Kaniso/Kiso: 1-1.2-1.4-1.6	Normal fault
6	$Vv/(1-Vh)$	Anisotropic	$Vv/Vh: 0.18-0.21-0.24-0.27$	Normal fault
7	θ_{inc}	Isotropic	$\theta_{inc}: 60-75-90-105-120$ (degree)	Normal fault
8	θ_{az}	Isotropic	$\theta_{az}: -30 -15 0 15 30$ (degree)	Normal fault

Case 1: σ_h/σ_v

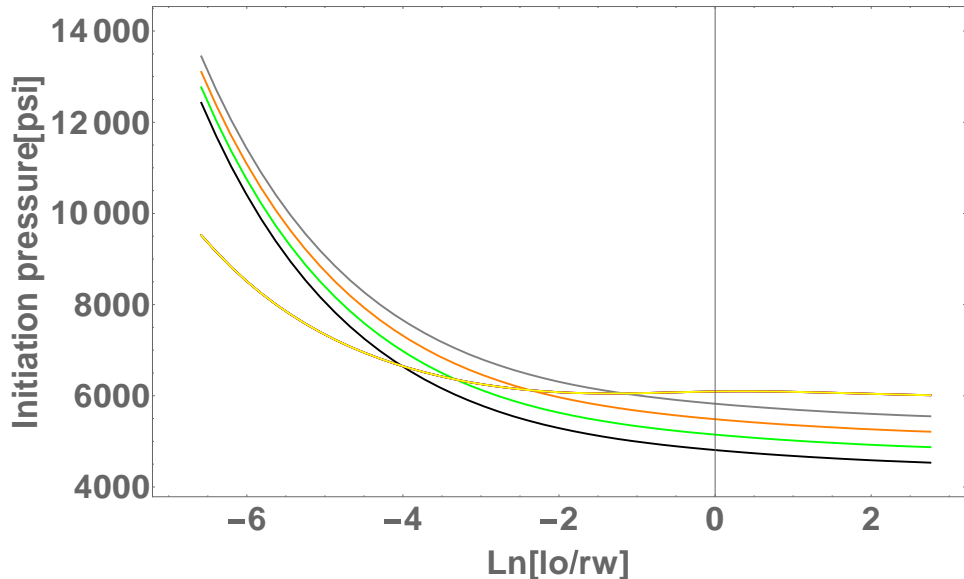
The change of minimum horizontal stress does not affect the initiation pressure of longitudinal fractures.

With the increase of minimum horizontal stress, the initiation pressure for transverse fractures is increasing and the critical length of perforation is also increasing.

When the minimum horizontal stress get more and more close to maximum horizontal stress, the initiation of longitudinal fracture becomes more favorable.



(a).



(b).

Case 1: σ_h/σ_v (FEDEM code)

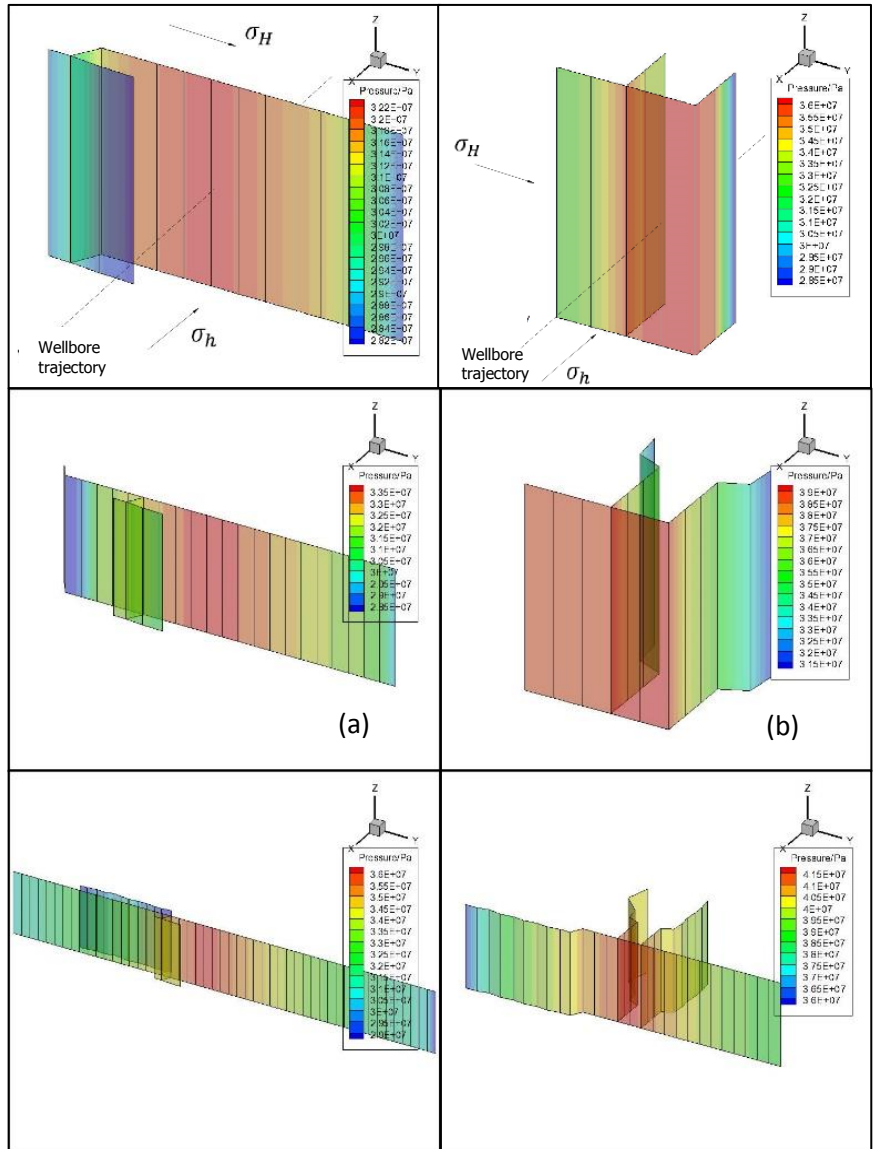
Perforation length= r_w	$\frac{\sigma_h}{\sigma_v} = 0.85$	$\frac{\sigma_h}{\sigma_v} = 0.65$
P_{ini} from FEDEM Model (psi)	5720.8	5236.2
P_{ini} from analytical Model (psi)	6054.8	5006.7
Favourable initial fracture pattern (FEDEM)	Longitudinal	Transverse
Favourable initial fracture pattern (Analytical)	Longitudinal	Transverse

Large $\frac{\sigma_h}{\sigma_v}$ ratio case ($\frac{\sigma_h}{\sigma_v} = 0.85$):

Fracture propagate along the wellbore at the beginning and propagate perpendicular to the wellbore afterwards.

Small $\frac{\sigma_h}{\sigma_v}$ ratio case ($\frac{\sigma_h}{\sigma_v} = 0.65$):

Fracture propagate perpendicular to the wellbore without creating any longitudinal fracture.



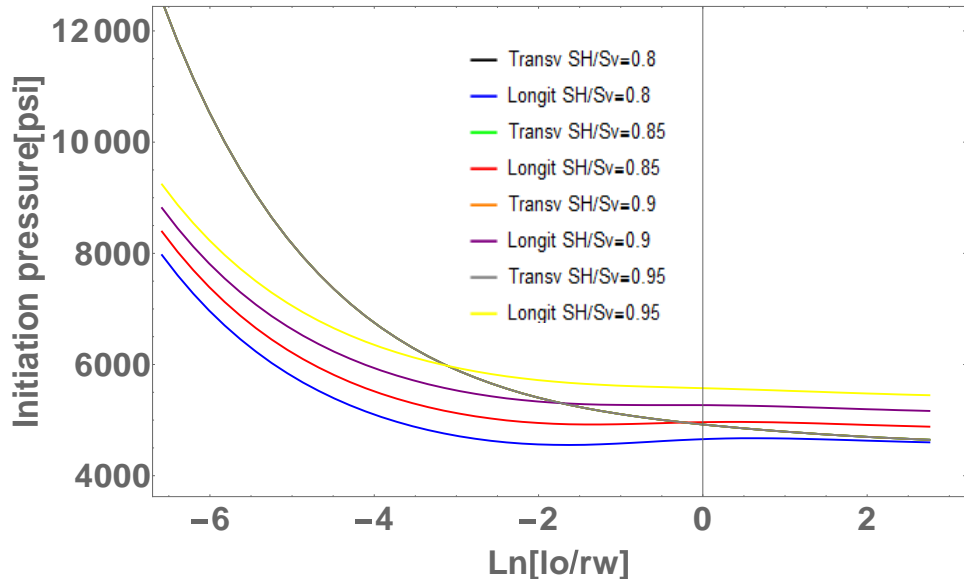
Schematic for fracture evolution in multiple stages:
(a). low $\frac{\sigma_h}{\sigma_v}$ ratio case; (b). high $\frac{\sigma_h}{\sigma_v}$ ratio case

Case 2: σ_H / σ_v

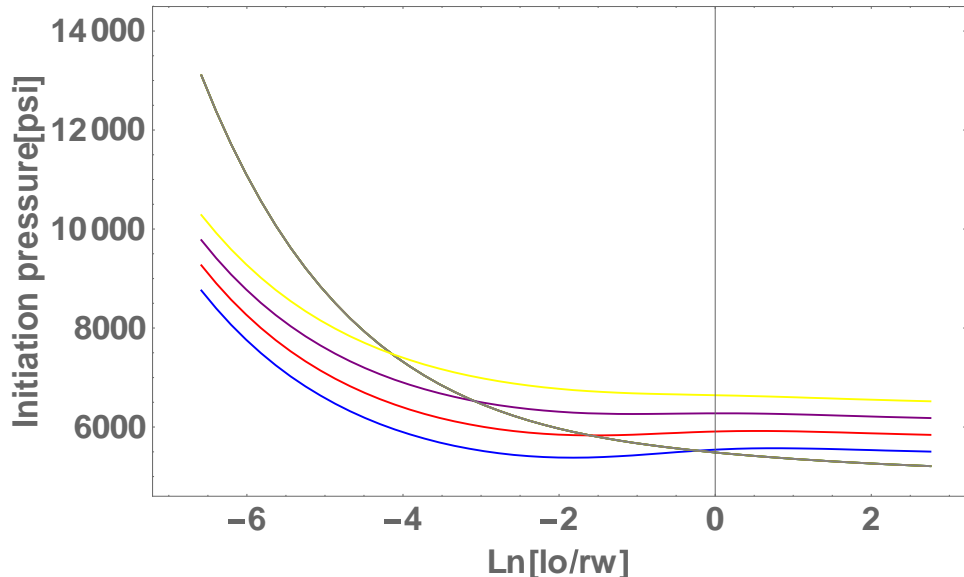
The change of maximum horizontal stress does not affect the initiation pressure of transverse fractures

With the increase of maximum horizontal stress, the initiation pressure for longitudinal fractures is increasing and the critical length of perforation is decreasing.

The initiation pressure for longitudinal fracture will reach to a minimum value which is even smaller than maximum horizontal stress for a specific perforation length



(a).



(b).

Case 2: σ_H/σ_v (FEDEM code)

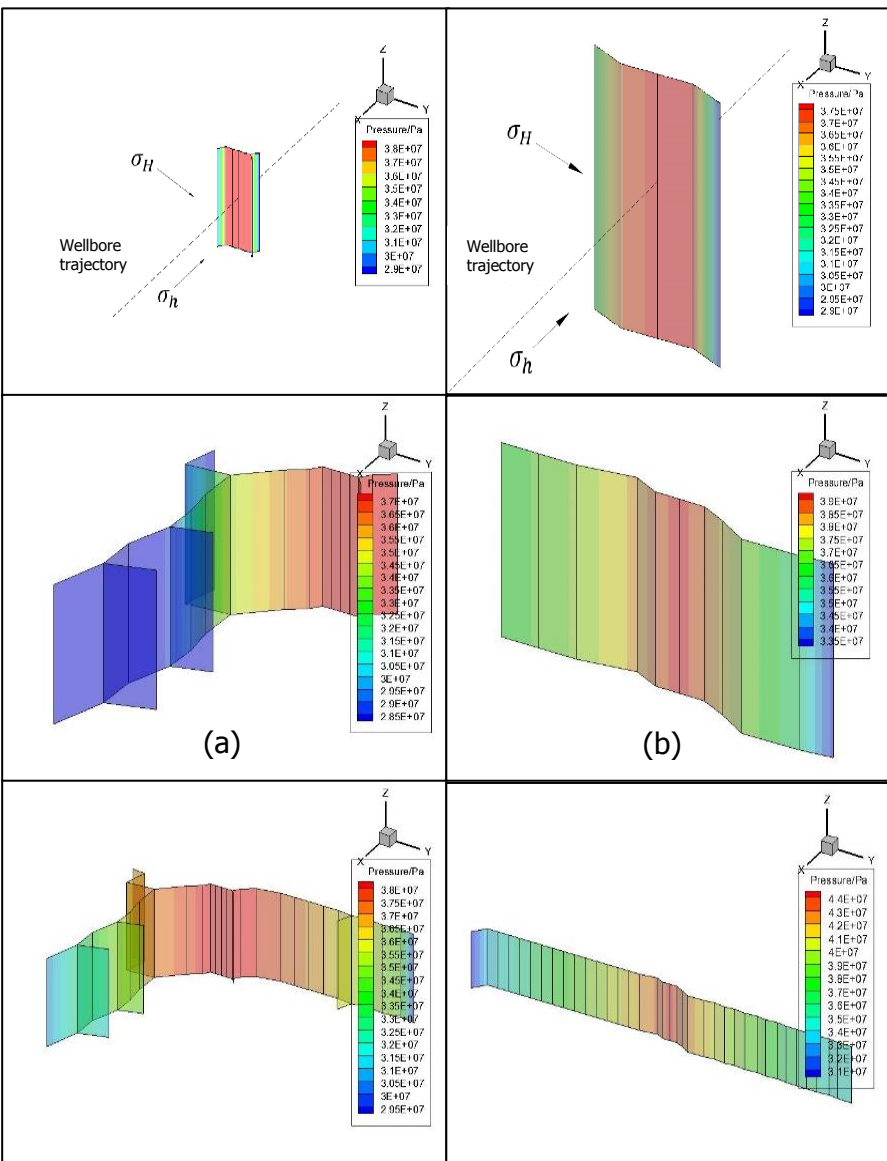
	$\frac{\sigma_H}{\sigma_v} = 0.8$	$\frac{\sigma_H}{\sigma_v} = 0.95$
P_{ini} from FEDEM Model (psi)	5308.4	5554.9
P_{ini} from analytical Model (psi)	5427.3	5684.7
Favourable initial fracture pattern (FEDEM)	Longitudinal	Transverse
Favourable initial fracture pattern (Analytical)	Longitudinal	Transverse

Large $\frac{\sigma_H}{\sigma_v}$ ratio case ($\frac{\sigma_H}{\sigma_v} = 0.95$):

Fracture propagate perpendicular to the wellbore without creating any longitudinal fracture

Small $\frac{\sigma_H}{\sigma_v}$ ratio case ($\frac{\sigma_H}{\sigma_v} = 0.8$):

Fracture propagate along the wellbore at the beginning and propagate perpendicular to the wellbore afterwards.



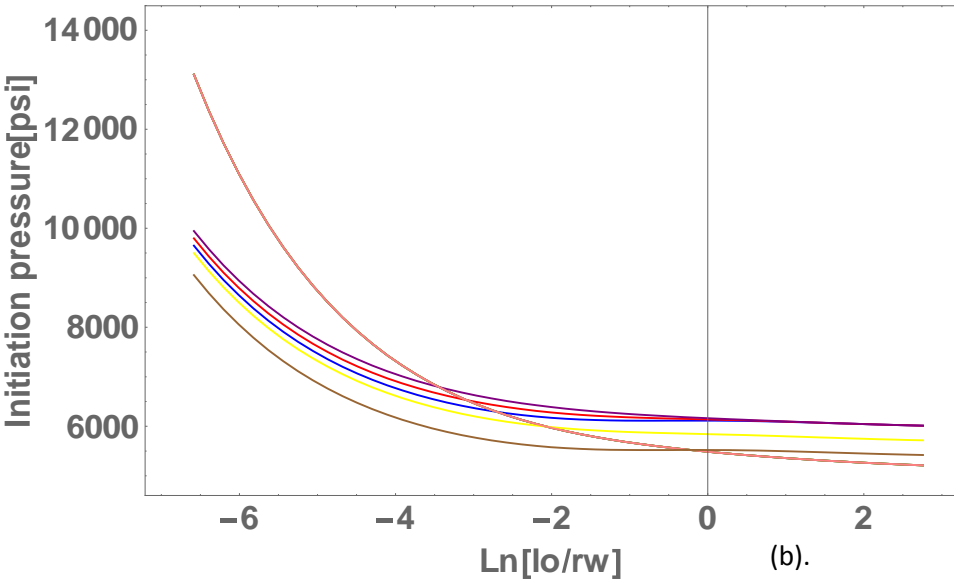
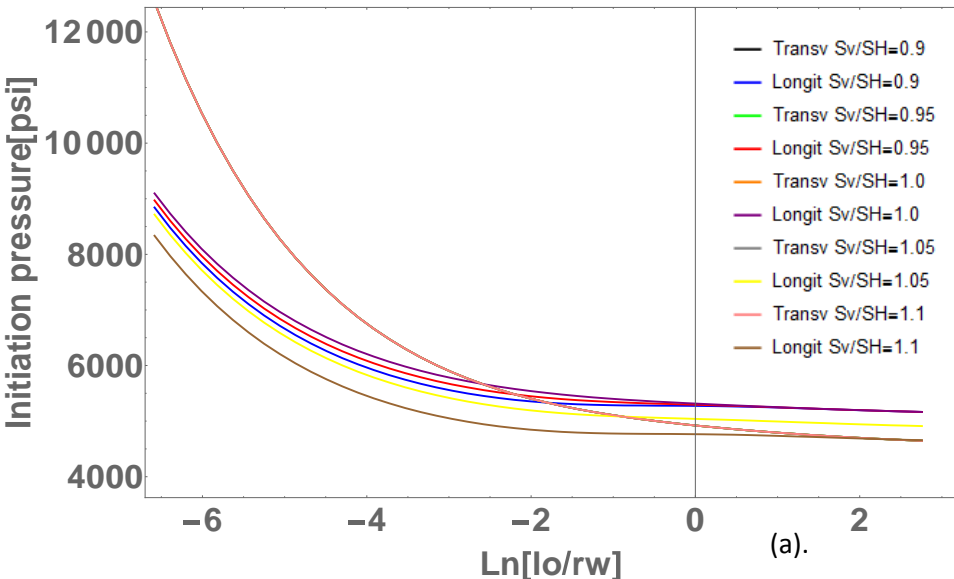
Schematic for fracture evolution in multiple stages:
(a). low $\frac{\sigma_H}{\sigma_v}$ ratio case; (b). high $\frac{\sigma_H}{\sigma_v}$ ratio case

Case 3: Normal fault -Strike Slip

The change of vertical stress has no effect on the initiation pressure of transverse fractures

For the vertical stress in normal fault stress region ($Sv > SH$), with the increase of vertical stress, the initiation pressure for longitudinal fractures decrease and the initiation pressure reaches maximum value when $Sv=SH$

When the vertical stress is in strike slip stress region ($SH > Sv$), with the increase of vertical stress, the initiation pressure for longitudinal fractures increase

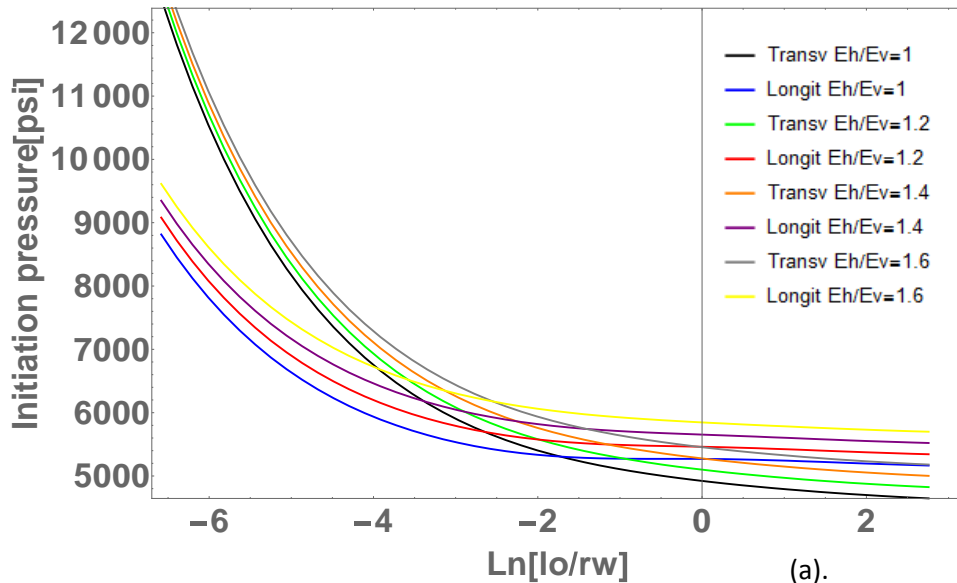


(a). Fayetteville and (b). Marcellus

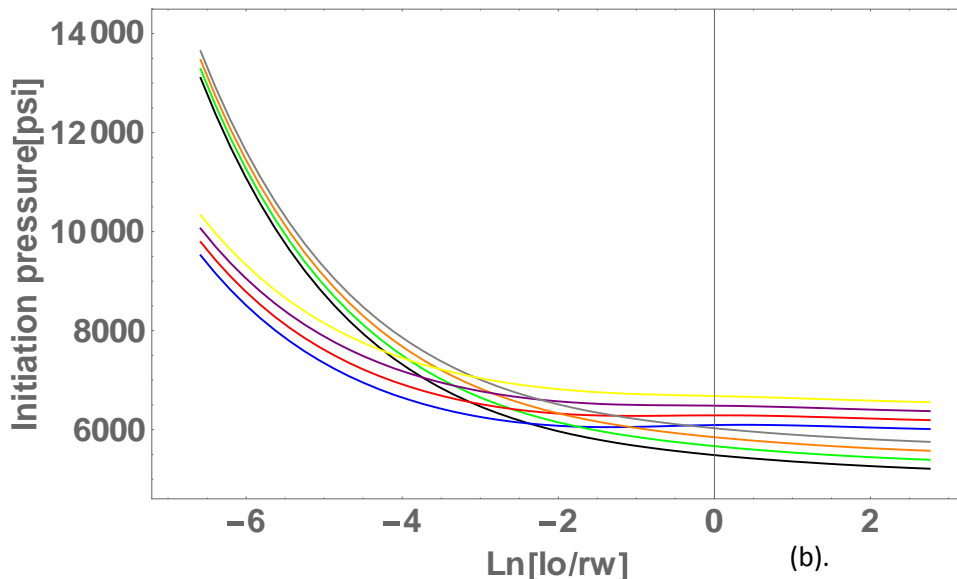
Case 4: E_h/E_v

The ratio of E_h/E_v affects initiation pressures for both transverse fractures and longitudinal fractures

With the increase of the ratio E_h/E_v , both the initiation pressures for transverse fractures and longitudinal fractures are increased



(a).



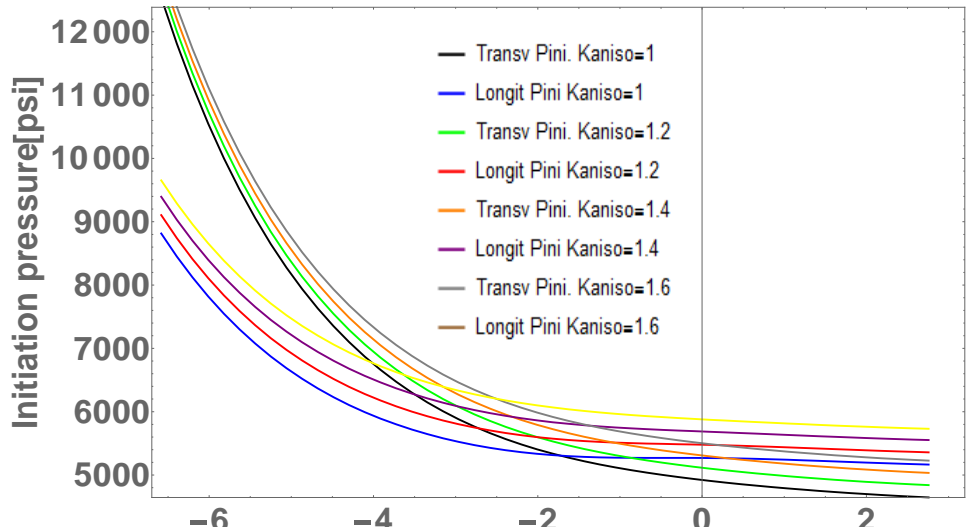
(b).

(a). Fayetteville and (b). Marcellus

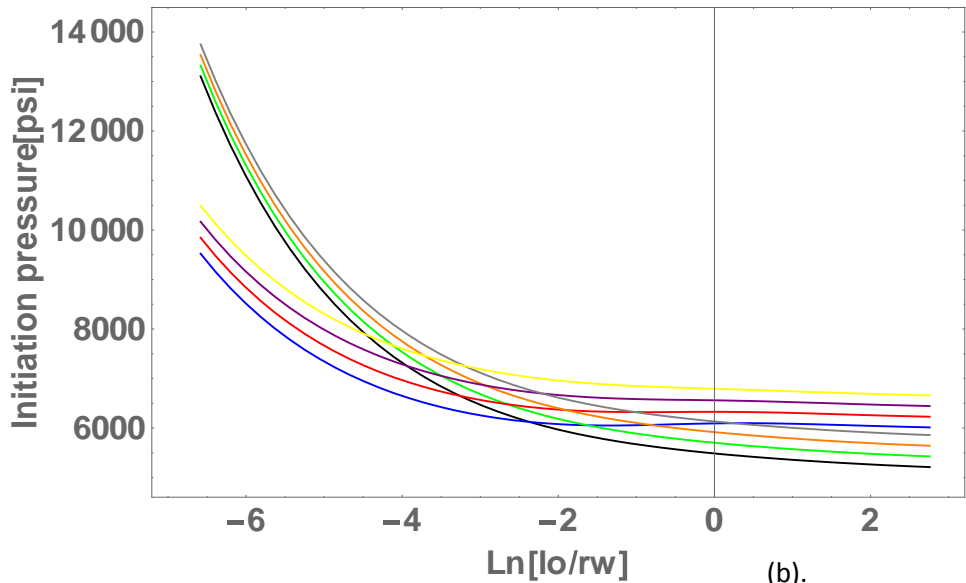
Case 5: K_{aniso}/K_{iso}

The ratio of K_{aniso}/K_{iso} affects initiation pressures for both transverse fractures and longitudinal fractures but has slightly effect on critical perforation length

For initiation pressures of both transverse fractures and longitudinal fractures, with the increase of K_{aniso} , the initiation pressure is increasing



(a).

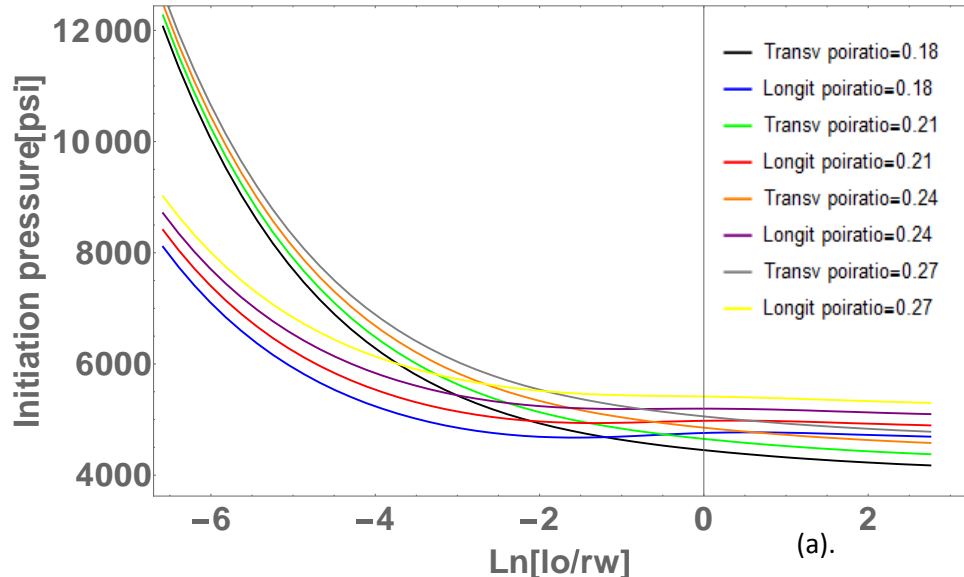


(b).

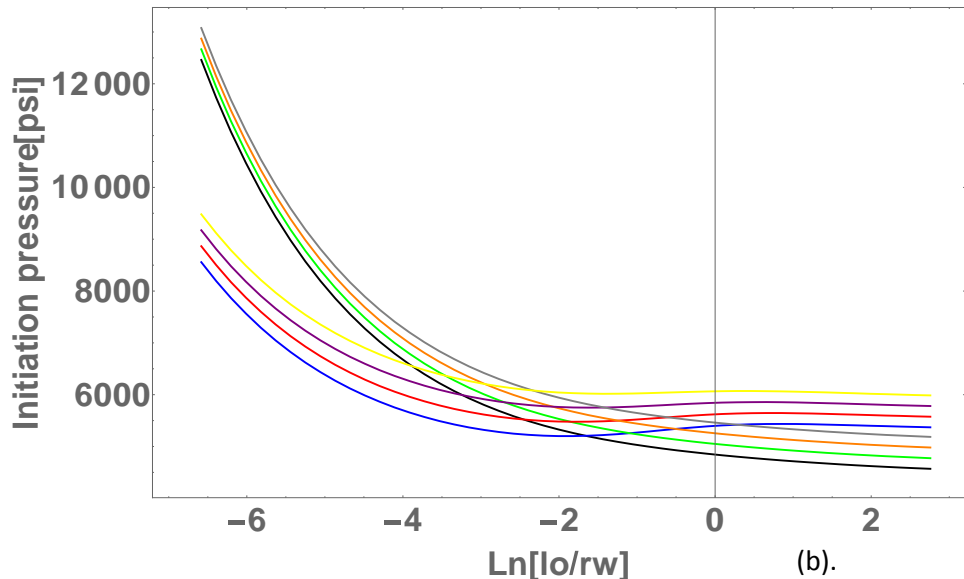
(a). Fayetteville and (b). Marcellus

Case 6: $V_v/(1-V_h)$

With the increase of $V_v/(1-V_h)$, the initiation pressures for both transverse fractures and longitudinal fractures are increased



(a).



(b).

(a). Fayetteville and (b). Marcellus

Case 7: Well deviation

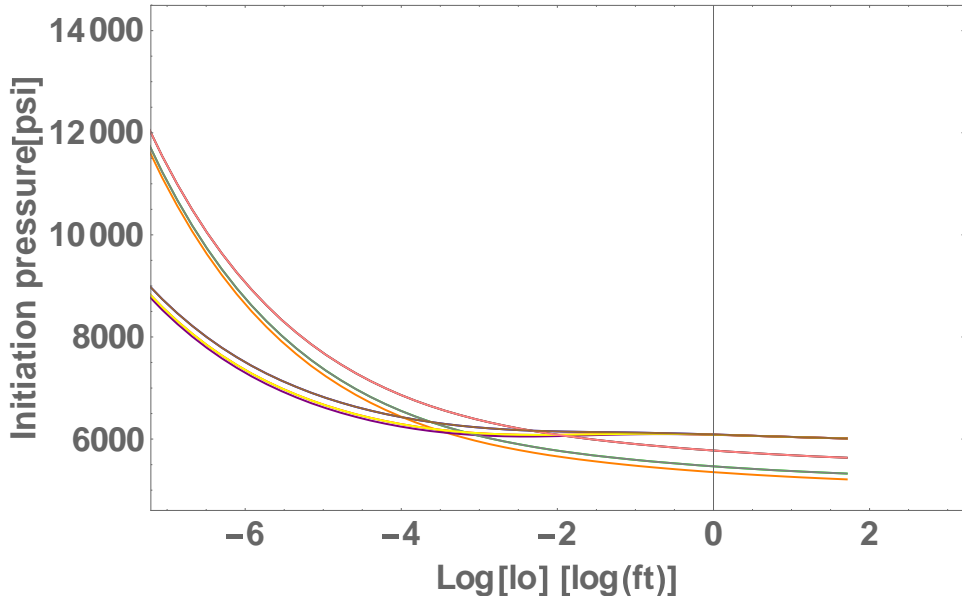
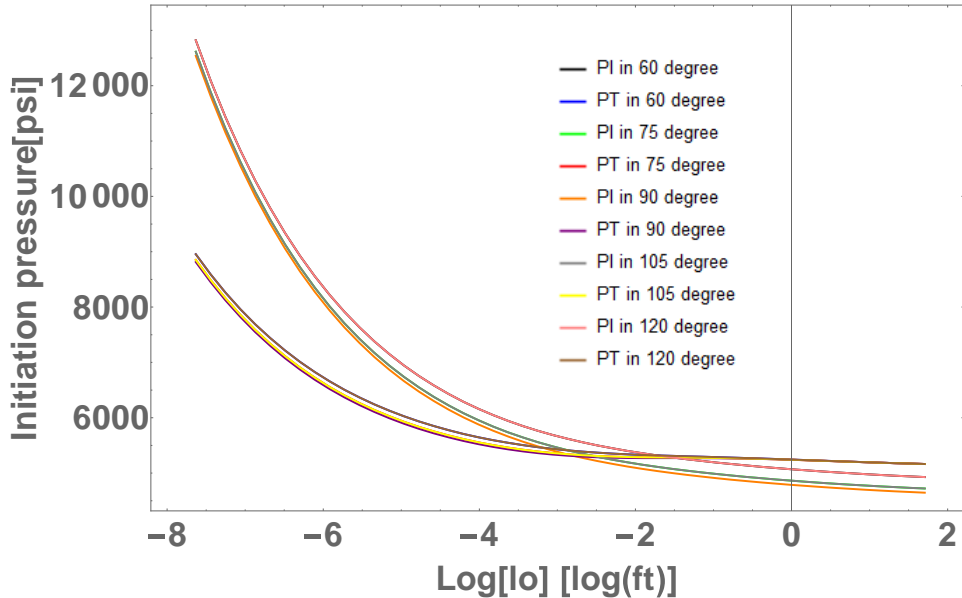
Inclination angle

θ_{az} is set to be 0 degree

Fracture initiation pressure reach minimum value when inclination angle is 90 degree for both fracture patterns

With the increase of deviation of inclination angle from 90 degree, the fracture initiation pressures for both pattern increase.

Well inclination angle has little effect on fracture initiation pressures



(a). Fayetteville and (b). Marcellus

Case 8: Well deviation

Azimuth angle

θ_{inc} is set to be 90 degree

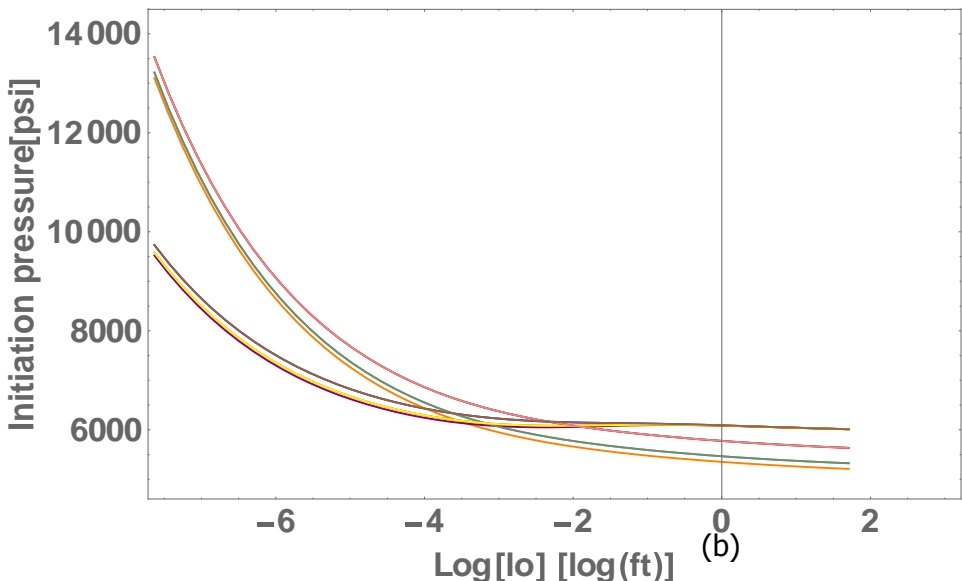
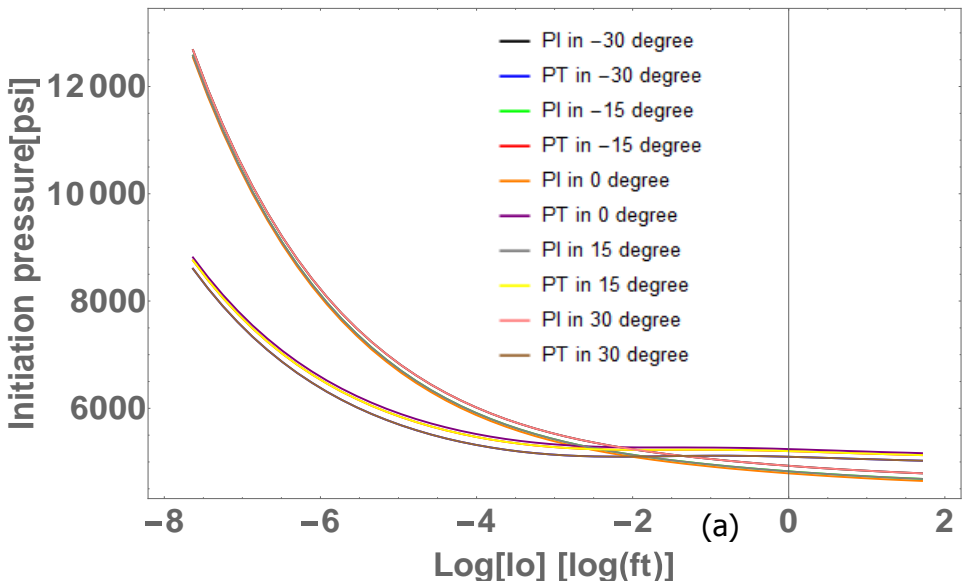
The initiation pressure reaches minimum value when azimuth angle equal to 0 degree for longitudinal fractures and reaches maximum value for transverse fractures

With the increase of the degree of deviation of azimuth angle from 0 degree, P_{ini} for longitudinal fractures increase and P_{ini} for transverse fractures decrease

The well azimuth angle also has little effect on fracture initiation pressures



(a). Fayetteville and (b). Marcellus



Conclusions

1. The elastic anisotropy of shale formation highly influence the calculation of geological stress distribution and fracture initiation prediction.
2. For the horizontal well parallel to the direction of minimum horizontal stress, transverse fracture initiation pressure is highly affected by minimum horizontal stress and longitudinal fracture initiation pressure is highly affected by maximum horizontal stress and vertical stress.
3. When the horizontal stress distributions close to isotropic stress condition ($\sigma_h \approx \sigma_H$), near-wellbore fracture geometry becomes complex and the initiation of longitudinal fractures become more favorable.
4. With the increase of formation anisotropy (K_{aniso}), the initiation pressures for both fracture patterns increase but it has negligible influence on critical perforation length.
5. With the increase of deviation of inclination angle from 90 degree, the fracture initiation pressures for both pattern increase. For azimuth angle, with the increase of the deviation of azimuth angle from 0 degree, the fracture initiation pressures for longitudinal fractures increase and the initiation pressure for transverse fractures decrease.

Thank you!

Contact: Han Li
Email: bhlihan@tamu.edu

